Boson peak in alkaline borate glasses: Raman spectroscopy, neutron scattering, and specific-heat measurements

G. D'Angelo,[1] G. Carini,[1] C. Crupi,[2] M. Koza,[3] G. Tripodo,[1] and C. Vasi[2]
[1]*Dipartimento di Fisica, University of Messina, 98166 Messina, Italy*
[2]*IPCF, CNR, 98158 Messina, Italy*
[3]*Institute Laue-Langevin, 38000 Grenoble, France*

(Received 30 July 2007; revised manuscript received 26 November 2007; published 26 January 2009)

The dependence of the boson peak on the alkaline ion in modified borate glasses $(M_2O)_{0.14}(B_2O_3)_{0.86}$ (M^+=Li^+,Na^+,K^+,Cs^+) was analyzed by performing Raman spectroscopy, inelastic neutron scattering, and low-temperature specific-heat measurements. It is found that the distribution of vibrations merging into the boson peak shifts to higher frequency by going from cesium to lithium. A linear correlation between the boson peak frequency and the transverse sound velocity is evidenced. The dependence on the polarizing power of the metallic cation is analyzed, stemming from considerations about elastic moduli. These findings suggest a mainly transverse character of the excess vibrational modes in glasses.

DOI: 10.1103/PhysRevB.79.014206 PACS number(s): 63.50.−x, 65.60.+a, 78.70.Nx, 78.30.−j

I. INTRODUCTION

It is well known that amorphous solids show universal characteristics in their low-frequency vibrational behavior not found in their crystalline counterparts. At temperatures below 30 K, the reduced specific heat C_p/T^3 of these systems exhibits a sizable hump[1] and it is appreciably greater than that evaluated by the continuum elastic prediction. This corresponds to an excess of low-energy vibrational states that are not accounted for by the Debye model.

In a more extended range of energy, below ~10 meV, inelastic neutron[2,3] and Raman-scattering[4,5] measurements reveal a strong broad band which can again be related to an excess of vibrational density of states (VDOS) $g(\omega)$. This bump is usually referred to as the "boson peak" (BP) because its intensity scales with temperature approximately according to the Bose-Einstein statistics. Nowadays, it represents almost a universal feature of disordered systems, being observed in most kind of glasses,[6] polymers,[7] and orientational glasses.[8]

However, although the boson peak shows properties, such as its shape, underlining the universality of some characteristics for the amorphous state, its frequency position and intensity depend strongly on the peculiar structure of the investigated system. As a matter of fact, the number of modes contributing to the BP results higher in strong[5] (like covalent systems) than in fragile[9] (molecular and ionic systems) glasses and, consequently, it is thought that the kind of chemical bonds influences the low-energy dynamics of glasses even if its effect in ruling the microscopic dynamics is obscure.

The boson peak occurrence is supposed to be strictly related to other universal properties of glasses, such as the thermal-conductivity plateau,[10] the local relaxation processes,[11] and the glass transition,[12] for which low-frequency excitations may play an important role. The interest concerning those unsolved questions gives reason for all experimental and theoretical efforts, which, however, have not led to a decisive conclusion about the microscopic origin of the BP.

In fact, in the past 20 years many experimental evidences and theoretical interpretations have shown the boson peak as due to phonon localization,[13] strong scattering caused either by elastic inhomogeneities[14] or by the presence of low-frequency excitations,[15] a marked bending of the dispersion curve of transverse modes,[16] a disorder induced version of a van Hove singularity,[17] soft anharmonic vibrations,[18] coupled rotation of tetrahedra[19] or intrinsically diffusive,[20] and propagating acoustic modes.[21] Furthermore, some models[22] suggest the existence of a strict connection between structural correlations observed on the mesoscopic length scale and low-energy dynamics since the wavelengths associated to low-frequency modes in amorphous systems lie just in this length scale.

Detailed information on the low-energy vibrational dynamics can be obtained by low-temperature specific heat and inelastic neutron scattering measurements, which allow the determination of the VDOS. Raman spectroscopy measurements, as well, represent a valuable mean to investigate low-frequency dynamics of amorphous systems. In fact, the disorder of the structure produces a breakdown in the selection rule of the wave vector ($\boldsymbol{Q}$), allowing all vibration modes to contribute to the Raman activity.[23] Consequently the low-frequency Raman scattering in glasses is related to the vibrational density of states, $g(\omega)$, by the following equation:[23,24]

$$I_R(\omega) = \frac{I_{\text{expt.}}\omega}{[n(\omega,T)+1]} = C(\omega)g(\omega), \qquad (1)$$

where I_R is the so-called reduced Raman intensity, $[n(\omega,T)+1]$ the Bose-Einstein population factor, $1/\omega$ the harmonic propagator, and $C(\omega)$ represents the light-vibration coupling coefficient, which turns out to have a complicated dependence on ω.[24]

As concerning the relation between structure and low-energy dynamics, it has to be considered that a great number of structural parameters (including connectivity, nature of intermolecular and intramolecular bonds, and spatial dimensionality) potentially attend in ruling the low-energy dynamics and it is a very complicated task to separate their specific

contribution and to establish the way and how much they influence the BP. Such difficulty can be get over by studying the vibrational dynamics in glasses in which the structural modifications are controlled and limited.

With regard to this problem, it is believed that modifications of the network structure caused by the introduction of alkali ions in borate glasses may provide clues on the BP origin. In alkaline borate glasses $(M_2O)_x(B_2O_3)_{1-x}$ (where M^+=Li^+,Na^+,K^+,Cs^+ and x is the molar fraction), in fact, by varying the network modifier M_2O, dramatic changes in the low-frequency dynamics just in the range of the boson peak are observed,[6,25] while the structural arrangement appears to be nearly unchanged. Many experimental results show that the structural changes taking place in the three-coordinated B_2O_3 glass by the addition of alkali oxides imply an increase in the number of four-coordinated borons at the expense of three-coordinated ones, with a progressive formation of various anionic borate structural groups.[26,27] The negative charge of the network sites is compensated by the positive charge of the metallic ions which do not participate in the network formation and which occupy interstitial voids. As a consequence the structure of modified borate glasses is essentially built up on covalently bonded structural units, while ionic bonds are made between M^+ and the B-O anionic units, the strength of which depends on the specific alkaline cation. The structural modifications following the addition of different alkali oxides are confined just in the low $\boldsymbol{Q}$ region ($\boldsymbol{Q}$ <2.5 Å^{-1}) of neutron-diffraction patterns,[28] while the high $\boldsymbol{Q}$ region ($\boldsymbol{Q}>2.5$ Å^{-1}) is almost insensitive to the alkali change.[29] These evidences imply that the presence of alkaline ions influences lengths beyond the nearest-neighbor distances but leaves unaffected the short-range order.

The present study is focused mainly on elucidating the influence of the peculiar cation-network interaction on the low-energy vibrational dynamics of alkaline borate glasses. For this aim, measurements of inelastic light and neutron scattering and low-temperature specific heat have been performed on $(M_2O)_{0.14}(B_2O_3)_{0.86}$ with M=Li,Na,K,Cs.

The remainder of the paper is divided into the following three sections. Section II describes the experimental details and Sec. III treats the experimental results, while in Sec. IV an analysis of data is reported. Finally, basic conclusions are given in Sec. V.

II. EXPERIMENTAL DETAILS

Alkaline borate glasses were obtained in the bulk and disk-shaped glasses with the composition x=0.14 by using, as starting materials, laboratory reagent 99.99% purity grades of boron oxide and alkaline nitrate. In all samples boron was isotopically enriched in ^{11}B (99%) in order to minimize the influence of the high neutron absorption of ^{10}B present in natural boron. All the glasses used in this study were prepared with high homogeneity and they were free from strains and bubbles. More specific details of the preparation procedure are described elsewhere.[30]

The Raman spectra were performed at room temperature on a double monocromator Jobin Yvon U-100 and were recorded in 90° scattering geometry in the HV (depolarized) and VV (polarized) configurations. Owing to the similar trends observed, in this paper only depolarized (VV) Raman spectra will be considered from here on. The incident light was the 5145 Å line of argon-ion laser and the power was kept below 300 mW. The accuracy of all stated measurements is within 1 cm^{-1}.

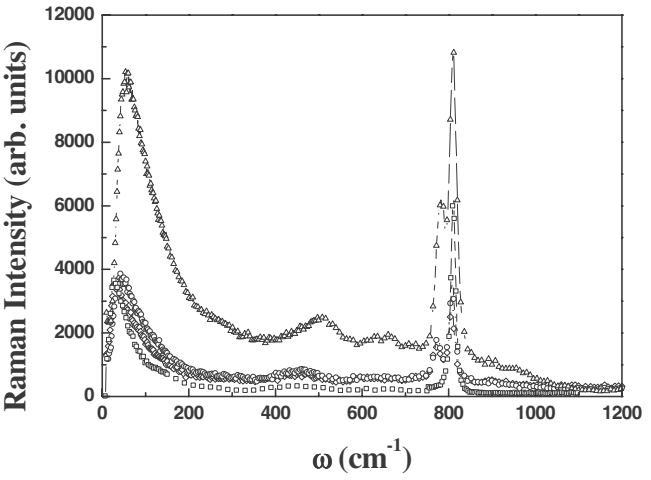

FIG. 1. Raman spectra of B_2O_3 (-□-), lithium (-△-), potassium (-○-), and cesium (-◇-) borate glasses at x=0.14 content.

The inelastic neutron scattering experiments were performed on the IN6 time-of-flight spectrometer at the Institut Laue-Langevin in Grenoble, with a neutron incident wavelength of λ=4.14 Å. The specimens were prepared in the form of disks approximately 50 mm in diameter and they were only 0.2 mm thick in order to limit the probability of multiple scattering. The generalized density of states $g(\omega)$ was determined after the usual data correction procedure, providing the subtraction of the empty cell, the normalization to vanadium, and the correction for absorption. Density of states on absolute scale was obtained by normalizing the low-energy spectra to the high-energy region between 25 and 120 meV, having made the assumption that alkaline cations do not contribute much to neutron signal in this spectral region.

The specific heat was measured using an automated calorimeter, which operates by the thermal relaxation method[31] using a silicon chip as the sample holder onto which a glass sample of about 10–30 mg was bonded by N-Apiezon grease. A surface mounting device resistor as temperature sensor and a Constantan strain gauge as heater element were attached to the other chip surface using a thermosetting resin. The density has been measured at room temperature by a Micrometrics Accupyc 1300 gas pycnometer under helium gas, having an accuracy of 0.03%.

III. EXPERIMENTAL RESULTS

A. Raman measurements

Figure 1 shows typical Raman spectra of pure boron oxide and alkaline borate glasses in the frequency range up to 1200 cm^{-1}. It can be observed that all spectra exhibit several bands, but a direct comparison between the different samples

TABLE I. Values of mass density ρ, boron atoms density ρ_B, frequency of the BP by Raman (ω'_{BP}) and neutron (ω_{BP}) scattering, and the temperature T_{max} of the bump in the C_P/T^3 of the studied glasses.

Sample	ρ (kg/m^3)	ρ_B (nm^{-3})	(ω'_{BP}) (cm^{-1})	ω_{BP} (cm^{-1})	T_{max} (K)
B_2O_3	1838	31.79	30.1		5.3[a]
$(Li_2O)_{0.14}(B_2O_3)_{0.86}$	2071	33.47	56.3	36.3	11.3
$(Na_2O)_{0.14}(B_2O_3)_{0.86}$				31.4	
$(Na_2O)_{0.16}(B_2O_3)_{0.84}$[b]	2122	31.37			10.6
$(K_2O)_{0.14}(B_2O_3)_{0.86}$	2088	29.59	43.6	26.3	8.3
$(Cs_2O)_{0.14}(B_2O_3)_{0.86}$	2484	25.88	33.0	19.0	6.4

[a]Reference 35.
[b]Reference 25.

is made difficult because the Raman intensity depends on the optical quality of samples. Consequently, an adequate normalization of raw data has been carried out to perform a quantitative analysis, as will be discussed in the following.

The spectrum of boron oxide is characterized by a strong, sharp, and highly polarized band at 806 cm^{-1} which has been assigned to a symmetric ring-breathing vibration of planar boroxol ring composed by three corner sharing BO_3 triangles.[32] This peak splits upon addition of alkaline oxide: the lowest-frequency band (at around 770 cm^{-1}) is associated to the breathing vibration of the six-membered rings containing both BO_3 triangles and BO_4 tetrahedra,[33] while the highest-frequency band (at around 804 cm^{-1}) arises, as in boron oxide, from breathing of boroxol rings built on BO_3 triangles. Moreover the amount of four-coordinated boron atoms is the same for glasses having the same concentration.[34] Therefore it is expected that, at a fixed concentration, the area A underlying the two bands lying in the range 750 cm$^{-1}<\omega<$850 cm^{-1} has to be constant since it represents an estimation of the fraction of three- and four-coordinated boron atoms. On these assessments, we have carried out the multistep normalization process of Raman data, as will be described in the following.

First, it has been subtracted to each spectrum a background corresponding to the value of the Raman intensity at the highest investigated frequency, i.e., the region where no molecular vibrations are revealed. Afterward the Raman data of all samples have been normalized to the ratio between the A values of each glass and that of B_2O_3. Finally, the obtained values have been divided by the numerical density of boron atoms ρ_B (see Table I) in order to account for the different number of scatterers per unit volume.

In Fig. 2 the normalized spectra for $\omega<150$ cm^{-1} are presented as $I_{expt.}/(\omega[n(\omega)+1])$ vs ω. According to Shuker and Gammon[23] [Eq. (1)] these spectra represent the product between the true vibrational densities of states as $g(\omega)/\omega^2$ and the coupling constant $C(\omega)$,

$$I_N(\omega)=\frac{I_{\text{expt.}}}{\omega[n(\omega,T)+1]}=\frac{C(\omega)g(\omega)}{\omega^2}. \quad (2)$$

We can observe that all investigated borate glasses show the presence of the boson peak, even though they exhibit spectral characteristic that appears to be dependent on the modifying oxide. Indeed, the magnitude of the maximum increases and its frequency position (see ω_{BP} values in Table I) decreases by going from lithium to cesium borate glass. Otherwise the high-frequency tail of the BP gets to the same value in all samples.

Moreover, an upturn is visible in the Raman intensity of all glasses in the frequency range below 20 cm^{-1}. It is the tail of the fast relaxation contribution, which dominates the Raman spectra of glasses mainly at very low frequency (below 10 cm^{-1}) and high temperatures.[36]

B. Inelastic neutron scattering measurements

The low-frequency vibrational densities of states derived by neutron scattering measurements, represented as $g(\omega)/\omega^2$, are shown in Fig. 3. The behaviors observed are once more characterized by an increasing BP intensity and a shift of its frequency position ω_{BP} to lower-frequency values by going from lithium to cesium glass and reflect mainly an increase in the density of states at low energy with decreasing polarizing power of alkali. By the comparison of Raman and neutron patterns, it is evident that the shapes of the spectra are similar, even though the ω'_{BP} values obtained by Raman measurements are always higher than those obtained by inelastic

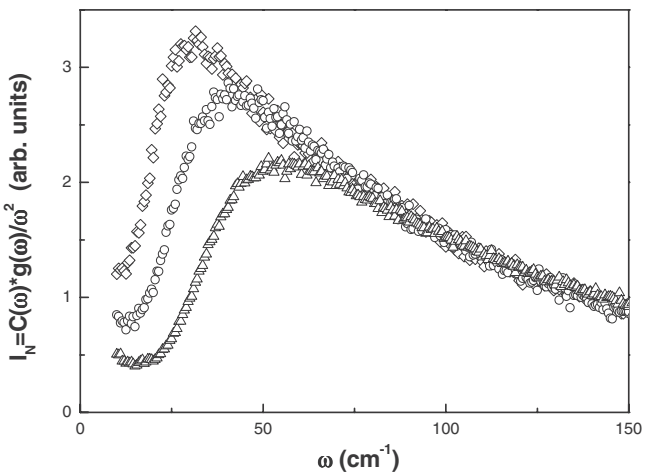

FIG. 2. Normalized Raman spectra of lithium (△), potassium (○), and cesium (◇) borate glasses in the BP region.

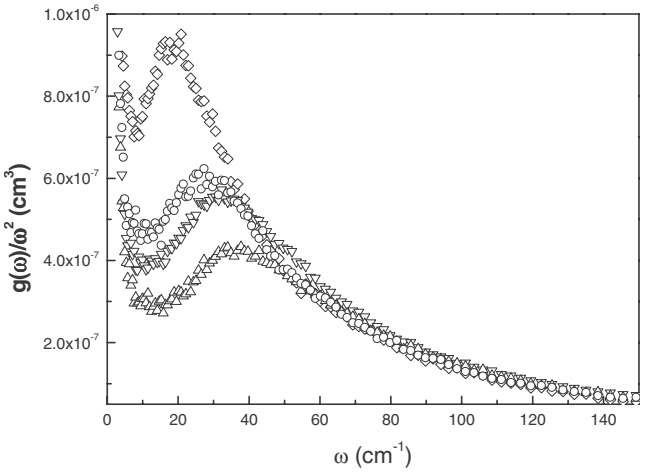

FIG. 3. Vibrational density of states $g(\omega)/\omega^2$ as a function of frequency for lithium (△), sodium (▽), potassium (○), and cesium (◇) borate glasses at the composition $x=0.14$.

neutron scattering, the reason being that the latter correspond to the maxima in $g(\omega)/\omega^2$, while the former do not since the phonon-photon coupling coefficient $C(\omega)$ is not constant but rather a monotonically increasing function of ω.

C. Specific-heat measurements

In Fig. 4 it is shown the temperature dependence of the reduced specific-heat C_p/T^3 data of lithium, potassium, and cesium borate glasses at the composition $x=0.14$. In the same figure it has been plotted also the data of sodium borate glass at $x=0.16$. This concentration, which we have traced in literature,[25] is not much far from the one we have investigated, making reasonable the comparison.

The behaviors revealed for all the samples show the existence of an upturn below $T=2.5$ K and a well-defined asymmetric broad peak which is the evidence of an excess C_p over

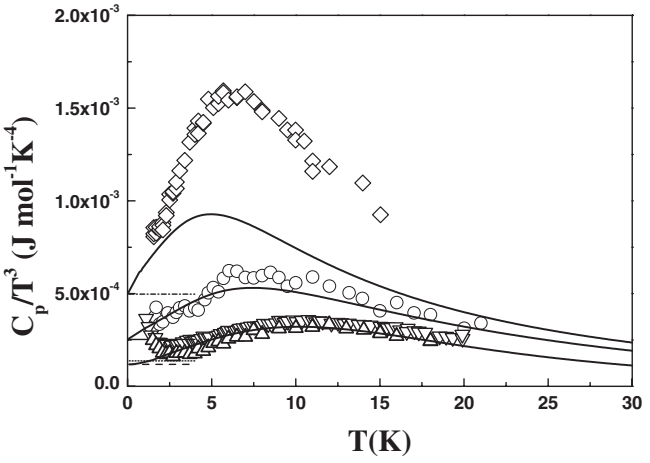

FIG. 4. Temperature dependence of the specific heat of lithium (△), sodium (▽), potassium (○), and cesium (◇) borate glasses and their Debye contribution plotted as dashed, dotted, solid, and short-dashed-dotted lines, respectively. The continuous solid lines represents the numerical evaluation of specific heat by Eq. (3).

the Debye contribution (see Fig. 4). The former contribution is usually ascribed to the existence of tunneling states in glasses,[37] the microscopic nature of which is still unknown. The treatment of this subject would require more accurate measurements at lower temperature and it is anyway beyond the topic of this paper.

The temperature T_{max} (see Table I) of the bump increases from about 6.4 up to 11.3 K, while its intensity decreases by going from cesium to lithium sample. Low-temperature specific heat and low-energy vibrational density of states are closely connected by the following equation:

$$C_p \approx C_V = 3Nk_B \int g(\omega)\left(\frac{\hbar\omega}{\kappa_B T}\right)^2 \frac{e^{(\hbar\omega/\kappa_B T)}}{[e^{(\hbar\omega/\kappa_B T)}-1]^2} d\omega, \quad (3)$$

where N is the Avogadro number and k_B is the Boltzmann constant. In particular, the position of the bump in the specific heat refers directly to the boson peak, being the equivalent in temperature of the BP energy in the dominant phonon approximation.

IV. DISCUSSION

The spectral shape of densities of states we have determined is in qualitative agreement with the specific-heat behavior. A large peak showing a widening on the descending side marks all the spectra (see Figs. 3 and 4). Moreover, the position and strength of peaks in $g(\omega)/\omega^2$ follow closely the changes with the alkaline cation displayed in the C_p/T^3 behaviors.

By using Eq. (3), the measured densities of vibrational states $g(\omega)$ have been used to calculate the specific heat as a function of temperature. In order to limit the intrusion of the wings of the elastic and quasielastic peaks on the vibrational contribution, the values for $g(\omega)$ below $\omega=0.5$ meV have been extrapolated to $\omega=0$, assuming an ω^2 dependence based on the Debye values derived from acoustic data. It is, in fact, known that both position and size of the bump C_p/T^3 have a high sensibility to the lowest-frequency data of VDOS.

The C_p/T^3 curves obtained numerically are compared with the calorimetric data in Fig. 4, where they are reported as solid lines. It is seen that the general features of the experimental curves are well reproduced, except for the cesium glass for which the numerical C_p/T^3 peak is smaller and its maximum is shifted to lower temperature.

The only feature that is not reproduced in the neutron spectra is the upturn that occurs in the experimental C_p/T^3 below 3 K, particularly evident in lithium and sodium glasses. In glasses the specific heat below 1 K is dominated by the contribution from two-level systems (TLSs), which shows a linear dependence on temperature.[37] Hence, the upturns we observe in C_p/T^3 represent the tail of this contribution and appear just in borate glasses where the boson peak is both not much high and shifted to higher temperatures. In the neutron spectra the TLS contribution is usually masked by the wings of the neutron elastic peak, being confined in the energy region below 0.5 meV. In the present case its absence in the numerical specific heat is an artifact of the extrapolation procedure, which could also be responsible for the scarce reproducibility of the cesium glass specific heat. In-

deed, in this sample the boson peak lies at very low frequencies, consequently important contribution of the low-frequency side of the peak could have been hugely underestimated by extrapolation. However, it cannot be excluded that the density of states obtained for Cs glass really describes a fewer number of vibrations than that contributing to the specific heat. This should imply that Cs ions are more directly involved in the dynamics of the boson peak and that the neutron intensity, and consequently the related VDOS, is low for the reason that the Cs neutron cross section is very low with respect to that of boron and oxygen, whose contributions dominate the neutron scattering. More detailed VDOS measurements at low frequencies as well as a neutron and specific-heat study of borate glasses with different content of Cs paralleled are necessary to clarify this point.

Concerning the Raman data, the comparison between the boson peak observed in Raman spectra and the C_p/T^3 data reveals a remarkable sensitivity of low-frequency Raman scattering to different alkaline cations. The frequency position of Raman peak ω'_{BP} and $T_{\max}$ change with the metallic cation size in a similar way, but the differences between the Raman intensities of different glasses in correspondence of the maximum are unusually small in proportion to those observed in the C_p data. That feature leads to believe that the inclusion of metallic cations of different ionic radii in the same borate matrix changes the strength of the phonon-photon coupling constant $C(\omega)$ in a nontrivial way. Notwithstanding, both low-energy Raman and neutron scattering spectra show maxima whose frequency increases with cation polarization power with the same rate of $T_{\max}$. Thus both experimental probes are sensitive to the same vibrations revealed in the specific-heat measurements. The question is to establish how much these techniques are potentially interchangeable in driving information about the boson peak in alkaline borate glasses.

Taking advantage of the availability of both neutron and Raman spectra, we have evaluated the Raman light-to-vibration coupling coefficient $C(\omega)$ by dividing the normalized Raman intensity I_N [Eq. (2)] by $g(\omega)/\omega^2$. The knowledge of the coupling coefficient $C(\omega)$ and that of its frequency dependence play a significant role for the topic of low-frequency vibrations because it contains information on the vibrational wave function[23] and consequently can make easier the identification of the modes involved in the ambiguous dynamics of the boson peak.

As a rule, very low-temperature light and neutron scattering data are used to evaluate $C(\omega)$ in order to avoid the influence of the quasielastic contribution. With respect to that question, we have to remark that, although the spectroscopic data reported in this study have been collected at room temperature, the quasielastic contribution decays so fast that it is negligible above 20 cm^{-1} for all glasses, making the following analysis reasonable. The coupling coefficients obtained for investigated samples are shown in Fig. 5.

All the samples show similar behaviors of $C(\omega)$. At frequencies lower than 20 cm^{-1} $C(\omega)$ keeps constant, then it increases quickly and subsequently exhibits a linear frequency dependence extending up to $\sim$150 cm^{-1}. Furthermore, the beginning of linear regime shifts to higher frequencies by going from Cs to Li glass. It is also observed that the

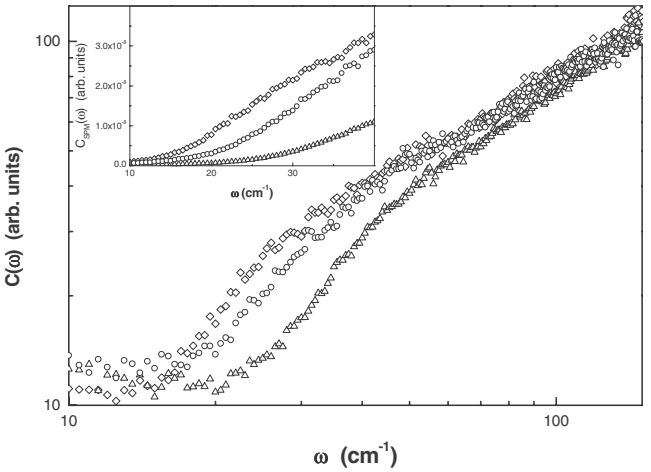

FIG. 5. The frequency dependence of the Raman coupling coefficient $C(\omega)$ of lithium (△), potassium (○), and cesium (◇) borate glasses. The inset shows the coupling coefficient for the soft-mode density of states of the same glasses (see text for details).

coupling coefficient is not the same for the samples: for a given frequency below 50 cm^{-1} the magnitude of $C(\omega)$ decreases by going from Cs to Li, leading to the same value at frequencies higher than 120 cm^{-1}. Concerning the $C(\omega)$ frequency behavior, the frequency region below 20 cm^{-1} will be kept out from the following analysis since it cannot be estimated the influence on $C(\omega)$ of the quasielastic contribution.

The linear behavior of $C(\omega)$ in the frequency interval between 35 and 150 cm^{-1} corresponds to the universally claimed linear frequency dependence.[38,39] The reason for this general linear dependence is not still clear, but it is accepted the idea that the generality implies that vibrations around the boson peak have the same nature in glasses and are not tied to the specifics of system, eventually being a vibration resulting by a strong hybridization or interrelation between different modes. However, this question is not yet completely settled and the possibility that two different kinds of vibrational excitations, each with its own $C(\omega)$, could coexist around the boson peak cannot be discarded, particularly in reason of recent hyper Raman-scattering results.[40] A constant value of $C(\omega)$ is invoked by different models[39,41] and associated to the existence of localized vibrations.

In the framework of soft potential model (SPM), the decrease in the vibrational density of states in the lower-energy region is explained by a decrease in the number of quasilocalized vibrations (soft modes) that are supposed to coexist with Debye-like acoustic phonons. In this model a constant value is expected for the coupling coefficient for the soft-mode density of states $C_{\mathrm{SPM}}(\omega)=I_R/[g(\omega)-g_D(\omega)]$, where $g_D(\omega)$ is the Debye density of states. In the inset of Fig. 5 it can be observed that $C_{\mathrm{SPM}}(\omega)$ shows a stronger frequency dependence than $C(\omega)$, in evident contrast with the SPM prediction. Therefore, we infer that in these glasses at the boson peak frequencies the separation between Debye-like acoustic vibrations and soft modes is highly questionable.

As concerning the linear frequency dependence of $C(\omega)$, it has recently shown that a broad set of different glasses can be scaled to a single master plot with a frequency depen-

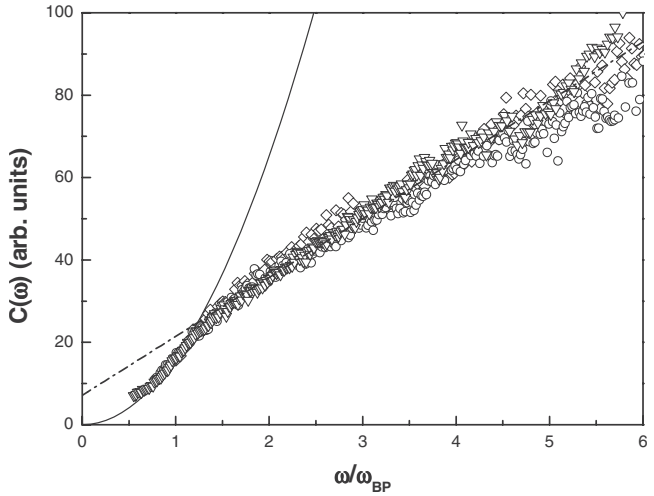

FIG. 6. Frequency dependence of the coupling coefficient $C(\omega)$ of lithium (△), potassium (○), and cesium (◇) borate glasses vs scaled frequency ω/ω_{BP}. The dashed-dotted line is a fit $C(\omega) \propto (\omega/\omega_{BP}+0.5)$. The solid line is a fit $C(\omega) \propto \omega^2$.

dence $C(\omega)=A(\omega/\omega_{BP}+B)$, where $B=0.5$ and ω_{BP} is defined as the position of maximum of $g(\omega)/\omega^2$. In Fig. 6 $C(\omega)$ for the investigated samples plotted against the scaled frequency ω/ω_{BP} is shown. In this plot the amplitudes of $C(\omega)$ have been normalized near $\omega/\omega_{BP}=1$. The most striking result is that, although the coupling coefficient shows some differences for borate glasses by changing the alkaline oxide (see Fig. 5), it falls onto a single spectral curve after the frequency is scaled by the boson peak position. More precisely, above the boson peak a linear behavior can be envisaged described by the equation $C(\omega)=A(\omega/\omega_{BP}+0.5)$ (showed in Fig. 6 as dashed-dotted line), while in the region around and below the BP ($\omega<1.2\ \omega_{BP}$) a superlinear behavior is traced deviating strongly from the extrapolation of linear behavior in analogy with the observation of Surovtsev and Sokolov.[39] A more accurate analysis reveals that the extrapolation of $C(\omega)$ to the limit $\omega \to 0$ appears to tend to the value $C(\omega)=0$ following a frequency dependence $C(\omega) \propto \omega^2$, as expected in the case of scattering from acousticlike vibrations[42] or from spatially attenuated acoustic waves.[43,44]

The change in $C(\omega)$ from parabolic to linear frequency dependence occurs at frequencies near the ω_{BP} for all borate glasses, indicating a wide participation at low frequencies of acoustic modes to the boson peak dynamics. The BP frequency marks the crossover to a different regime, where localized and extended or diffusive excitations plausibly coexist; the first contributing with a $C(\omega)=$const and the latter originating the linear dependence.

The linear dependence extends up to very high frequency, where strong deviation was observed in other glasses.[39] Moreover, all borate glasses show very similar behavior. This result finds an explanation by considering that it is expected that high-frequency vibrations depend on the atomic structure of glass, which is the same for the investigated glasses.

All these considerations on the frequency dependence of the coupling coefficient lead to the conclusion that the boson peak wave functions are very similar in alkaline borate glasses and are hence unaffected by the metallic cations.

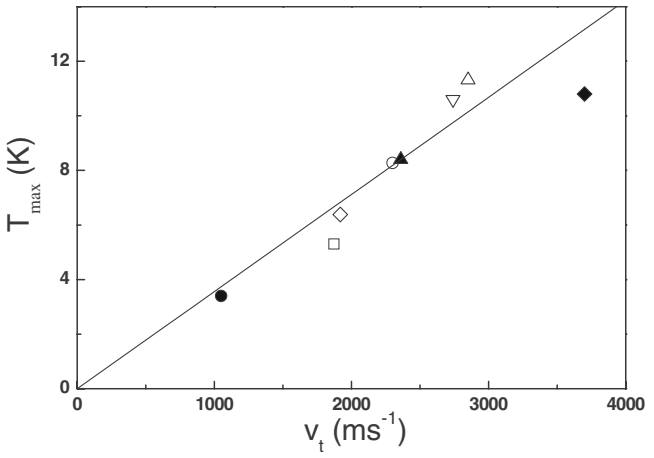

FIG. 7. Temperature T_{max} of the bump in the C_p/T^3 as a function of transverse velocity for boron oxide (□), lithium (△), sodium (▽), potassium (○), and cesium (◇) borate glasses. In the same figure the data of Se (●), (Refs. 48 and 49), GeO_2 (▲) (Refs. 48 and 50), and SiO_2 (◆) (Refs. 48 and 51) are also reported.

Concerning the boson peak, different hypotheses have been advanced about its origin, ascribing it to van Hove singularities which are located at high-symmetry points at the boundaries of the first Brillouin zone[17] or to the existence of a strongly dispersive transverse-acoustic branch.[45] Moreover recent measurements on metallic glasses have pointed out a possible relation between the boson peak strength and the elastic moduli.[46]

What is more, the temperature position of the peak in the reduced low-temperature specific heat for many crystalline and glassy systems has been related to the crossover frequency, ω_{co}, where the Debye and the effective experimental VDOS cross for the first time.[47] The crossover frequency ω_{co} should correspond to the Brillouin-zone-boundary frequency for shear waves and the following equation is derived for elastically isotropic glasses:

$$\omega_{co} = \left(\frac{2}{\pi}\right)\left(\frac{C_{44}}{\rho}\right)^{1/2} K_{BZ}, \tag{4}$$

where ρ is the density, C_{44} is the elastic constant for pure transverse waves, and K_{BZ} is the wave vector magnitude at the end of the first pseudo-Brillouin zone.

Equation (4) should imply a linear correspondence between the frequency of the boson peak and the transverse velocity v_t since $C_{44}=(\rho v_t^2)$. In the attempt to verify this assessment, the dependence of T_{max} on the shear velocity v_t has been investigated in alkaline borate glasses and is shown in Fig. 7.

As it is possible to observe in Fig. 7 the prediction of Eq. (4) is confirmed. By going from cesium to lithium, the temperature of the bump in C_p/T^3 increases linearly with v_t. This relation keeps its validity also when it is extended to a wide group of glasses, appearing as a promising general feature of glasses.

Another important observation is that in these glasses the longitudinal sound velocity is related to the transverse component by the relation $v_l \sim 1.8 v_t$. In the light of these results,

TABLE II. Values of transverse (v_t) and longitudinal (v_l) velocity, shear (G) and bulk (B) modulus, Young's modulus (Y) determined by ultrasonic measurements, coordination number, ionic radius, and Debye temperature Θ_D of the glasses under study.

Sample	v_t (m/s)	v_l (m/s)	G (GPa)	B (GPa)	Y (GPa)	Coordination number	Ionic radius (Å)	Θ_D (K)
B_2O_3	1872	3367	6.6	12.5	17.3			267
$(Li_2O)_{0.14}(B_2O_3)_{0.86}$	2851	5160	16.8	32.6	44.1	4[a]	0.73	427
$(Na_2O)_{0.16}(B_2O_3)_{0.84}$	2760[b]	5100[b]	15.9	33.9	42.4	6[c]	1.16	405[d]
$(K_2O)_{0.14}(B_2O_3)_{0.86}$	2301	4228	11.1	22.6	29.3	8[e]	1.52	332
$(Cs_2O)_{0.14}(B_2O_3)_{0.86}$	1919	3525	9.2	18.7	24.3	9[f]	1.8	265

[a]Reference 52.
[b]Reference 56.
[c]Reference 53.
[d]Reference 25.
[e]Reference 54.
[f]Reference 55.

it is believed that transverse modes are directly involved in the boson peak dynamics settling its position, while the asymmetric shape of the boson peak appearing as a broadening on its right tail (clearly visible in Figs. 2 and 3) can be considered as the clue of the involvement of longitudinal modes, which are expected to contribute at higher frequencies and temperatures.

Since the structure of the investigated glasses and the atomic forces inside and between the structural units have to be considered basically the same, the strong differences in the vibrational dynamics and sound velocities could be ascribed to the effect of the electrostatic interactions between alkalis lying inside interstitial voids and the surrounding B-O atoms. Indeed, notwithstanding alkaline ions have got an identical charge, they are characterized by a different polarization ability, which regulates the formation of bonds of different strength between the metallic cation and the surrounding anionic groups. In particular, both the size of the first coordination sphere and the coordination number increase by going from lithium to cesium (see Table II) and thus the same electric charge of the alkaline ion will be distributed to different numbers of anions. Hence, due to the size of alkaline cations, the network site will be polarized as a function of ionic radius leading to different distances of the cation charge within the site. The polarization yields to a Coulombian interaction and therefore a potential energy gradient, the strength of which will strictly depend on cation size.

More detailed information about the nature of molecular bonds can be inferred by the elastic moduli. The elastic bulk modulus (B), Young's modulus (Y), and shear modulus (G) of the investigated glasses have been determined (see Table II) from the experimental values of density ρ, longitudinal velocity (v_l), and shear velocity (v_t), using the Lamè coefficients $\lambda=\rho(v_l^2-v_t^2)$ and $\mu=\rho v_t^2$ through the following standard relations and are listed in Table II:

$$Y = \mu\frac{(3\lambda + 2\mu)}{(\lambda + \mu)}, \tag{5}$$

$$B = \frac{(3\lambda + 2\mu)}{3}, \tag{6}$$

$$G = \mu. \tag{7}$$

We have to observe that the densities of all investigated glasses are higher than that of pure B_2O_3 and increase with increasing ionic radius of alkali ions. Differently the values of molar volume are lower than that of B_2O_3 glass, with the exception of Cs glass and increase from lithium to cesium sample. In particular, in lithium and sodium glasses the introduction of the metallic oxide leads to a decrease in molecular weight; thus, the increase in densities arises from a strong volume contraction. This volume contraction can be attributed to the interatomic forces between the modifying cations which fill the interstices of the glass network and the glass-forming anions. By increasing the ionic radius the strength of interaction forces decreases, leading to a volume contraction gradually decreasing. Moreover the measured shear, bulk, and Young's moduli follow the same trend of ultrasonic velocities with modifying cations. The reduced resistance to shear with increasing ionic radius could arise from an increased loose structure of glasses containing heavy alkali ions.

According to the model proposed by Bridge and Higazy,[57] the bulk modulus of the glass network depends on both the cross-link density (defined as the number of bridging bonds per network forming cation) and the bond-stretching force constant. In alkali borate glasses, the addition of M_2O to boron oxide results in an increase in the three-dimensional linkage due to the transformation of threefold-coordinated borons into fourfold-coordinated ones. At fixed concentration of M_2O, the same increase in dimensionality is foreseen for different alkali cations, which contributes to increase both sound velocity and bulk modulus. As a consequence the differences in the bulk modulus observed in the investigated glasses should arise from marked differences in the bond-stretching force constants, related to the ionic linkage be-

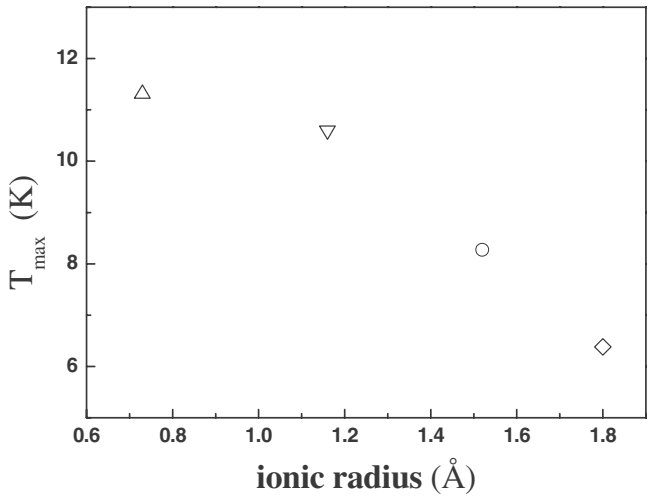

FIG. 8. Temperature T_{max} of the bump in the specific heat as a function of ionic radius for lithium (△), sodium (▽), potassium (○), and cesium (◇) borate glasses.

tween M^+ and the B-O anionic units, the strength of which depends on the specific alkaline cation.

The increasing value of the polarizing ability of alkaline cations by going from cesium to lithium implies a growing strength of interaction between alkalis and their first-nearest anionic structural units. As a consequence, the B-O environment overlooking interstitial voids filled with alkalis undergoes a progressively stronger strain.

In Fig. 8 T_{max} as a function of ionic radius values (see Table II) provided by Shannon[58] is shown. The finding of higher values of the peak temperature in correspondence of smaller alkali size reveals a strong sensitivity of the boson peak modes to the structural scale involving the cation-site force fields.

Taking these results into consideration, it can be believed that vibrations merging into the boson peak arise from low atomic density regions which host alkaline cations and that they are strongly influenced by constraints imposed by the alkalis on transverse displacements of structural units overlooking these voids. The decrease in the intensity of the boson peak, clearly observable in Figs. 2–4, would be the natural consequence of a transfer toward higher frequencies of these modes. Alkaline ions making stronger Coulombian bonds give rise to a greater shifting and to a considerable reduction in the amount of low-energy vibrations. Moreover, by increasing the metallic oxide content, it is expected the transfer of a greater number of these excitations. Such a hypothesis is confirmed by the experimental evidence of a decreased specific heat in sodium[25] and lithium borate glasses[28].

V. CONCLUSIONS

The dependence of the boson peak on the alkaline ion in modified borate glasses $(M_2O)_{0.14}(B_2O_3)_{0.86}$ $(M^+ = Li^+, Na^+, K^+, Cs^+)$ was analyzed by performing Raman, neutron scattering, and low-temperature specific-heat measurements. Results show that the introduction of different alkalis in borate matrix leads to strong changes in the low-frequency vibrational dynamics. By going from cesium to lithium through potassium glass, the boson peak decreases its magnitude and shifts to higher frequency or temperature. A clear correlation between the temperature of the maximum in C_p/T^3 and the transverse sound velocity is found. The Raman coefficient $C(\omega)$ has been evaluated and it appears basically the same for all glasses. Moreover it is demonstrated that $C(\omega)$ has a linear dependence on frequency $C(\omega) \propto (\omega/\omega_{BP}+0.5)$ above the boson peak maximum and a superlinear behavior at frequencies below ω_{BP}. It is believed that vibrations merging into the boson peak arise from low atomic density regions which host alkaline cations and that they are strongly influenced by constraints imposed by the alkalis on transverse displacements of structural units overlooking these voids.

[1] W. A. Phillips, *Amorphous Solids: Low-Temperature Properties* (Springer, Berlin, 1981).
[2] U. Buchenau, N. Nücker, and A. J. Dianoux, Phys. Rev. Lett. **53**, 2316 (1984); U. Buchenau, M. Prager, N. Nücker, A. J. Dianoux, N. Ahmad, and W. A. Phillips, Phys. Rev. B **34**, 5665 (1986).
[3] D. Engberg, A. Wischnewski, U. Buchenau, L. Börjesson, A. J. Dianoux, A. P. Sokolov, and L. M. Torell, Phys. Rev. B **58**, 9087 (1998); **59**, 4053 (1999).
[4] J. Schroeder, W. Wu, J. L. Apkarian, M. Lee, L. G. Hwa, and C. T. Moynihan, J. Non-Cryst. Solids **349**, 88 (2004).
[5] A. P. Sokolov, E. Rössler, A. Kisliuk, and D. Quitmann, Phys. Rev. Lett. **71**, 2062 (1993).
[6] S. Kojima and M. Kodama, Physica B **263-264**, 336 (1999).
[7] B. Frick and D. Richter, Science **267**, 1939 (1995).
[8] M. Ramos, S. Vieira, F. Bermejo, J. Dawidowski, H. E. Fisher, H. Schober, M. Gonzalez, C. K. Loong, and D. L. Price, Phys. Rev. Lett. **78**, 82 (1997).
[9] U. Buchenau, Prog. Theor. Phys. Suppl. **126**, 151 (1997).
[10] B. Rufflé, G. Guimbetrière, E. Courtens, R. Vacher, and G. Monaco, Phys. Rev. Lett. **96**, 045502 (2006); D. A. Parshin and C. Laermans, Phys. Rev. B **63**, 132203 (2001).
[11] H. R. Schober, J. Phys.: Condens. Matter **16**, S2659 (2004).
[12] A. G. Kalampounias, S. N. Yannopoulos, and G. N. Papatheodorou, J. Non-Cryst. Solids **352**, 4619 (2006).
[13] Yu. G. Vainer, A. V. Naumov, M. Bauer, and L. Kador, Phys. Rev. Lett. **97**, 185501 (2006); M. I. Klinger and L. Vatova, Phys. Rev. B **72**, 134206 (2005).
[14] W. Schirmacher, G. Diezmann, and C. Ganter, Phys. Rev. Lett. **81**, 136 (1998).
[15] V. G. Karpov, M. I. Klinger, and F. N. Ignatiev, Sov. Phys. JETP **57**, 439 (1983); A. Il'in, V. G. Karpov, and D. A. Parshin, *ibid.* **65**, 165 (1987).
[16] S. N. Taraskin and S. R. Elliott, Europhys. Lett. **39**, 37 (1997);

M. T. Dove, M. J. Harris, A. C. Hannon, J. M. Parker, I. P. Swainson, and M. Gambhir, Phys. Rev. Lett. **78**, 1070 (1997).
[17] S. I. Simdyankin, S. N. Taraskin, M. Elenius, S. R. Elliott, and M. Dzugutov, Phys. Rev. B **65**, 104302 (2002); S. N. Taraskin, Y. L. Loh, G. Natarajan, and S. R. Elliott, Phys. Rev. Lett. **86**, 1255 (2001).
[18] U. Buchenau, Yu. M. Galperin, V. L. Gurevich, D. A. Parshin, M. A. Ramos, and H. R. Schober, Phys. Rev. B **46**, 2798 (1992).
[19] U. Buchenau, H. M. Zhou, N. Nucker, K. S. Gilroy, and W. A. Phillips, Phys. Rev. Lett. **60**, 1318 (1988).
[20] P. B. Allen and J. L. Feldman, Phys. Rev. B **48**, 12581 (1993); Phys. Rev. Lett. **62**, 645 (1989); J. Fabian and P. B. Allen, *ibid.* **77**, 3839 (1996).
[21] P. Benassi, M. Krisch, C. Masciovecchio, V. Mazzacurati, G. Monaco, G. Rocco, F. Sette, and R. Verbeni, Phys. Rev. Lett. **77**, 3835 (1996).
[22] S. R. Elliott, Europhys. Lett. **19**, 201 (1992); A. P. Sokolov, A. Kisliuk, M. Soltwisch, and D. Quitmann, Phys. Rev. Lett. **69**, 1540 (1992).
[23] R. Shuker and R. W. Gammon, Phys. Rev. Lett. **25**, 222 (1970).
[24] F. L. Galeneer and P. N. Sen, Phys. Rev. B **17**, 1928 (1978).
[25] E. S. Pinango, M. A. Ramos, R. Villar, and S. Vieira, in *Basic Features of the Glassy State*, edited by J. Colmenero and A. Alegria (World Scientific, Singapore, 1990), p. 514.
[26] B. N. Meera and J. Ramakrishna, J. Non-Cryst. Solids **159**, 1 (1993); E. I. Kamitsos, A. P. Patsis, M. A. Karakassides, and G. D. Chryssikos, *ibid.* **126**, 52 (1990).
[27] F. L. Galeener, G. Lukovsky, and J. C. Mikkelsen, Phys. Rev. B **22**, 3983 (1980).
[28] C. Crupi, Ph.D. thesis, Università di Messina, 2007.
[29] L. Börjesson, R. L. MsGreevy, and W. S. Howells, Philos. Mag. B **65**, 261 (1992); J. Swenson, L. Börjesson, and W. S. Howells, Phys. Rev. B **52**, 9310 (1995).
[30] G. Carini, G. Carini, G. D'Angelo, G. Tripodo, A. Bartolotta, and G. Salvato, Phys. Rev. B **72**, 014201 (2005).
[31] G. Carini, G. D'Angelo, S. Interdonato, G. Salvato, and G. Tripodo, Atti Accad. Peloritana Pericolanti, Cl. Sci. Fis., Mat. Nat. **72**, 329 (1994).
[32] P. A. V. Johnson, A. C. Wright, and R. N. Sinclair, J. Non-Cryst. Solids **50**, 281 (1982); A. C. Hannon, R. N. Sinclair, J. A. Blackman, A. C. Wright, and F. L. Galeener, *ibid.* **106**, 116 (1988).
[33] B. P. Dwivedi, M. H. Rahman, Y. Kumar, and B. N. Khanna, J. Phys. Chem. Solids **54**, 621 (1993).
[34] J. Zhong and P. J. Bray, J. Non-Cryst. Solids **111**, 67 (1989).
[35] G. K. White, S. J. Collocott, and J. S. Cook, Phys. Rev. B **29**, 4778 (1984).
[36] L. Saviot, E. Duval, N. V. Surovtsev, J. F. Jal, and A. J. Dianoux, Phys. Rev. B **60**, 18 (1999).
[37] R. O. Pohl, in *Amorphous Solids: Low Temperature Properties*, edited by A. W. Phillips (Springer, Berlin, 1981).
[38] A. Fontana, R. Dell'Anna, M. Montagna, F. Rossi, G. Viliani, G. Ruocco, M. Sampoli, U. Buchenau, and A. Wischnewski, Europhys. Lett. **47**, 56 (1999).
[39] N. V. Surovtsev and A. P. Sokolov, Phys. Rev. B **66**, 054205 (2002).
[40] B. Hehlen, E. Courtens, R. Vacher, A. Yamanaka, M. Kataoka, and K. Inoue, Phys. Rev. Lett. **84**, 5355 (2000); G. Simon, B. Hehlen, E. Courtens, E. Longueteau, and R. Vacher, *ibid.* **96**, 105502 (2006).
[41] V. L. Gurevich, D. A. Parshin, J. Pelous, and H. R. Schober, Phys. Rev. B **48**, 16318 (1993).
[42] A. J. Martin and W. Brenig, Phys. Status Solidi B **64**, 163 (1974).
[43] J. Jäckle, in *Amorphous Solids: Low-Temperature Properties*, edited by W. A. Phillips (Springer, Berlin, 1981).
[44] E. Duval, L. Saviot, N. Surovtsev, J. Wiedersich, and A. J. Dianoux, Philos. Mag. B **79**, 2051 (1999).
[45] M. J. Harris, S. M. Bennington, M. T. Dove, and J. M. Parker, Physica B **263-264**, 357 (1999).
[46] Y. Li, H. Y. Bai, W. H. Wang, and K. Samwer, Phys. Rev. B **74**, 052201 (2006).
[47] D. J. Safarik, R. B. Schwarz, and M. F. Hundley, Phys. Rev. Lett. **96**, 195902 (2006).
[48] R. O. Pohl, X. Liu, and E. Thompson, Rev. Mod. Phys. **74**, 991 (2002).
[49] J. C. Lasjaunias and R. Maynard, J. Non-Cryst. Solids **6**, 101 (1971).
[50] A. P. Jeapes, A. J. Leadbetter, C. G. Waterfield, and K. E. Wycherley, Philos. Mag. **29**, 803 (1974).
[51] P. Flubacher, A. J. Leadbetter, J. A. Morrison, and B. P. Stoicheft, J. Phys. Chem. Solids **12**, 53 (1959).
[52] J. Aidong, L. Shirong, H. Qingzhen, C. Tianbin, and K. Deming, Acta Crystallogr., Sect. C: Cryst. Struct. Commun. **46**, 1999 (1990).
[53] N. Penin, M. Touboul, and G. Nowogrocki, J. Alloys Compd. **363**, 104 (2004).
[54] J. Krogh-Moe, Acta Crystallogr., Sect. B: Struct. Crystallogr. Cryst. Chem. **30**, 1827 (1974).
[55] N. Penin, L. Segin, M. Touboul, and G. Nowogrocki, Solid State Sci. **4**, 67 (2002).
[56] J. T. Krause and C. R. Kurjian in *Borate Glasses*, edited by L. D. Pye, V. D. Frechette, and N. J. Kreidl (Plenum, New York, 1978), Vol. 12, p. 577.
[57] B. Bridge and A. Higazy, Phys. Chem. Glasses **27**, 1 (1986).
[58] R. D. Shannon, Acta Crystallogr., Sect. A: Cryst. Phys., Diffr., Theor. Gen. Crystallogr. **32**, 751 (1976).